Mat. Res. Soc. Symp. Proc. Vol. 756 © 2003 Materials Research Society 

# Cation Transport and Surface Reconstruction in Lanthanum Doped Strontium Titanate at High Temperatures

Karsten Gömann[1], Günter Borchardt[1], Anissa Gunhold[2], Wolfgang Maus-Friedrichs[2], Bernard Lesage[3], Odile Kaïtasov[4], Horst Baumann[5]
[1]Institut für Metallurgie, Technische Universität Clausthal, Robert-Koch-Str. 42, D-38678 Clausthal-Zellerfeld, Germany
[2]Institut für Physik und Physikalische Technologien, Technische Universität Clausthal, Leibnizstr. 4, D-38678 Clausthal-Zellerfeld, Germany
[3]Laboratoire d'Etude des Matériaux Hors Equilibre, Université Paris-Sud, F-91405 Orsay Cedex, France
[4]Centre de Spectrométrie Nucléaire et de Spectrométrie de Masse, Université Paris-Sud, F-91405 Orsay Cedex, France
[5]Institut für Kernphysik, J. W. Goethe-Universität, August-Euler-Str. 6, D-60486 Frankfurt, Germany

## ABSTRACT

Tracer diffusion experiments were carried out in synthetic air at 1573 K in $SrTiO_3$(100) and (110) single crystals, which were either undoped or doped with up to 1 at.% La, respectively. Tracer sources of $^{139}$La and $^{142}$Nd were applied by ion implantation. The resulting depth profiles were measured by SIMS. The reconstruction of the surface was monitored ex-situ using microscopic and spectroscopic methods including SEM, EPMA, and AFM. The measured tracer diffusivities show no dependency on orientation. The tracer diffusion takes place via cation vacancies. Under oxidizing conditions the dopant is compensated by Sr vacancies. Hence the diffusion is increasing strongly with La concentration. The observed time dependency of the diffusivities may be related to a space charge layer postulated by the current defect chemistry model for donor doped $SrTiO_3$. At high dopant concentrations annealing leads to segregation of bulk La to the surface. La is not significantly incorporated into the secondary crystallites at the surface which consist almost entirely of Sr and O.

## INTRODUCTION

Donor doped strontium titanate $SrTiO_3$ is a promising material for resistive oxygen sensors operated at high temperature. Changing the ambient oxygen partial pressure $p(O_2)$ under high temperature leads to an undesirable surface reconstruction and the formation of secondary phases. Though an overall consistent model is still lacking, many of the phenomena can be explained by the bulk defect chemistry model of donor doped $SrTiO_3$ [1]. The defect chemistry is dominated by the following reaction (see [2] for defect notation):

$$V_O^{\bullet\bullet} + 2e' + \frac{1}{2}O_{2(g)} \Leftrightarrow O_O^x \qquad (1)$$

Upon oxidation of O deficient crystals, $V_O^{\bullet\bullet}$ and free electrons are consumed by the incorporation of O into the lattice. Finally, Sr vacancies are generated and a subsequent change in

the donor compensation mechanism occurs. The excess Sr migrates to the surface where secondary $SrO_x$ phases are formed on top of the surface (e.g. [3,4]), and Ruddlesden-Popper phases ($SrO{\cdot}nSrTiO_3$, [5]) are formed at the surface between the islands [6]:

$$Sr_{Sr}^{x} + 2e' + \frac{1}{2}O_{2(g)} \Leftrightarrow V_{Sr}^{''} + SrO_{sec.phase} \qquad (2)$$

The amount of $V_{Sr}^{''}$ produced is fixed by the donor content

$$[D^{\bullet}] = 2[V_{Sr}^{''}], \qquad (3)$$

explaining the correlation of secondary phase quantity and dopant concentration. A recent extension of the model introduces a space charge zone in the near surface region based on the strong differences in point defect mobility [7]. At low $p(O_2)$, $O_2$ is released into the atmosphere yielding a large number of electrons, which partly reduce $Ti^{4+}$, resulting in the formation of $Ti^{3+}$ containing phases like $Ti_2O_3$ or $LaTiO_3$ [8-10].

For a model verification, the diffusivities of the involved species must be known. Recent studies obtain a depth-dependent O tracer diffusion coefficient which is attributed to a gradient in $[V_O^{\bullet\bullet}]$ in the surface near space charge region [7,11]. From the O diffusion data, a $V_{Sr}^{''}$ diffusion coefficient was deduced, which is in acceptable accordance to a measured value [12]. Yet, except for one publication on Sr and Ti diffusion in undoped $SrTiO_3$ at 2148 K [13] and one computer simulation study [14], no data on cation diffusivities in $SrTiO_3$ is published. The work presented here is part of a larger study where diffusion experiments are combined with investigations of the topography, chemistry and electronic structure of the reconstructed surface in order to establish a kinetic model for the secondary phase formation on donor doped $SrTiO_3$. Here, we will present new results on the secondary phase growth and La and Nd diffusion experiments under oxidizing conditions.

## EXPERIMENTAL

$SrTiO_3$(100) and (110) single crystals with La contents of 0, 0.02, 0.2, and 1 at.% were obtained from Crystec (Germany). The crystals were grown under reducing conditions. The samples were annealed at ambient pressure in a flow of synthetic air (80 % $N_2$, 20 % $O_2$) for up to 6 weeks at 1573 K to equilibrate the samples to a sufficient depth with the atmosphere. During the first hours the experiments were suspended several times to monitor the surface reconstruction ex situ with various methods including Scanning Electron Microscopy (SEM), Atomic Force Microscopy (AFM), and Electron Probe Microanalysis (EPMA). Additional analyses were performed at the end of the equilibration step.

Prior to tracer deposition the 5 % -doped samples were washed for 24 h at 60 °C in $H_2O_{deion}$, hereby removing most of the secondary phases. The tracer sources were deposited by ion implantation using a mass separated and scanned ion beam. $^{139}La^{+}$ ions were implanted with a dose of $1\times10^{16}$ $cm^{-2}$ at 40 or 120 keV, $^{142}Nd^{+}$ ions were implanted with a dose of $2\times10^{15}$ $cm^{-2}$ at 120 keV. Diffusion annealing took place under the same conditions as in the equilibration step. The depth profiles were analyzed with SIMS (Cameca IMS3f), using a scanned (250 × 250 $\mu m^2$) 10 kV $O^-$ beam at a current of 100 nA. The crater depth was measured with a surface profilometer (Tencor AlphaStep 500).

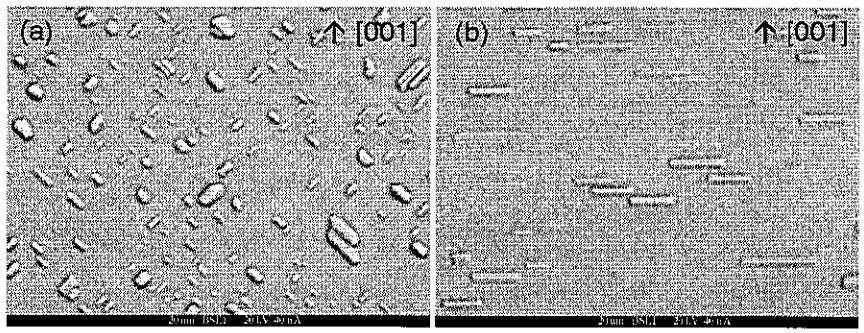


**Figure 1.** SEM backscattered electron images. 1 at.% La-doped $SrTiO_3$ annealed for 40.5 d at 1573 K in synthetic air. (a) (100) surface, (b) (110) surface.

## RESULTS AND DISCUSSION

### Surface Reconstruction

Annealing of donor doped $SrTiO_3$ in oxidizing atmosphere leads to the formation of $SrO_x$ phases on top of the surface [3,4]. At 1573 K, already after 1 hour a significant island growth is visible, which seems to be largely completed after 1 day of annealing. Fig. 1 shows backscattered electron images of the annealed surfaces. On the (100) surface the crystallites grow epitaxially in an angle of 45° to the $SrTiO_3$ lattice, reducing the misfit of the SrO (cubic, d = 0.51 nm) and $SrTiO_3$ (cubic, d = 0.391 nm) lattices to 7 %. On the (110) surface the growth is oriented perpendicular to the [001] axis, resulting in the same misfit value. EPMA investigations of 1 at.% La-doped samples confirm that the islands contain Sr, but no Ti. In contrast to earlier observations [15], also La concentrations of 0.5 at.% were measured, which corresponds to half of the initial La content of the $SrTiO_3$ crystal. The composition of the islands is the same on both surfaces. On the less doped samples similar secondary phases are formed, but number and size of the islands decrease substantially with the donor content. On the surface surrounding the islands of the (100) oriented crystal, terrace-like structures with step heights of typically several Å are observed with AFM [6]. In contrast, the (110) surface is heavily reconstructed, forming ridges and trenches oriented along the [001] direction perpendicular to the secondary phases.

Fig. 2 shows SIMS depth profiles after the equilibration annealing. At high dopant concentrations the thermal treatment leads to the migration of La to the surface. This segregation may result from the gradient in $V_{Sr}''$ in the postulated space charge layer [7]. As the depth distribution of the dopant was considered constant in the model [7], the effect of this observation on the validity of the model will have to be evaluated.

### Tracer Diffusion Experiments

Ion implanted depth profiles show a Gaussian distribution [16]. Diffusion of the implanted tracer leads to a broadening of the Gaussian profile. The diffusivities are determined by fitting the appropriate solution of Fick's second law to the profiles, which in this case is written as

$$c(x,t) = \frac{N}{\sqrt{2\pi(\Delta R_p^2 + 2Dt)}} \exp\left(-\frac{(x-R_p)^2}{2\Delta R_p^2 + 4Dt}\right), \qquad (4)$$

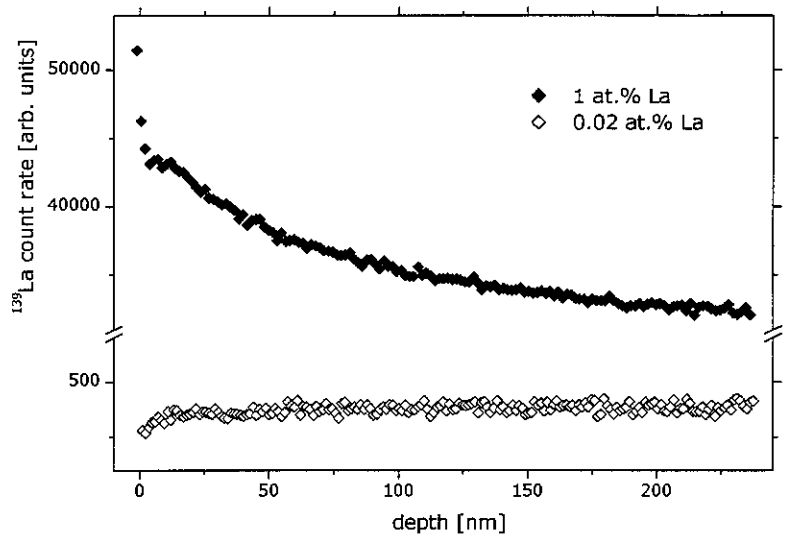


**Figure 2.** SIMS La depth profiles. 0.02 and 1 at.% La-doped $SrTiO_3(100)$ annealed for 40.5 d at 1573 K in synthetic air.

with c being the concentration, x the depth, t the time, N the implanted dose, $\Delta R_p$ the standard deviation of the initial distribution, $R_p$ the mean value of the projected range, and D the diffusion coefficient. Hence, the diffusion coefficient is derived directly from the increase in $\Delta R_p$ after the annealing experiment.

Fig. 3(a) shows representative La tracer depth profiles implanted at 120 keV. As a result of ion beam mixing during the SIMS analysis, the profile measured after implantation deviates slightly from the Gaussian shape. This is visible only in the low concentration region and has no significant influence on the determination of $\Delta R_p$. After thermal treatment, the concentration maximum is shifted to lower depth values. Several explanations are possible: Predominantly Sr might evaporate from the surface, as was observed by [3]. Furthermore, material may also be consumed during the secondary phase growth. Lastly, such a shift is also observed when the tracer ions are reflected at the surface.

During implantation, radiation damage is introduced into the lattice with a depth distribution comparable to the implanted ions, but shifted in direction of the surface. On annealing this may result in extended defects like clusters, causing differing tracer diffusivities in this layer. To check for the influence of beam damage, experiments with Nd implantation were also carried out. As Nd is not contained in the samples, a lower fluence is sufficient to obtain a satisfactory dynamic range for the experiment. Like La, Nd occurs predominantly in trivalent state and has a comparable ionic radius and mass. The Nd depth profiles in Fig. 3(b) show that the Nd ions are reflected at the surface. The case of reflection is solved mathematically by adding a second exponential term to the Gaussian function:

$$c(x,t) = \frac{N}{\sqrt{2\pi(\Delta R_p^2 + 2Dt)}}\left\{\exp\left(-\frac{(x-R_p)^2}{2\Delta R_p^2 + 4Dt}\right) + \exp\left(-\frac{(x+R_p)^2}{2\Delta R_p^2 + 4Dt}\right)\right\} \qquad (5)$$

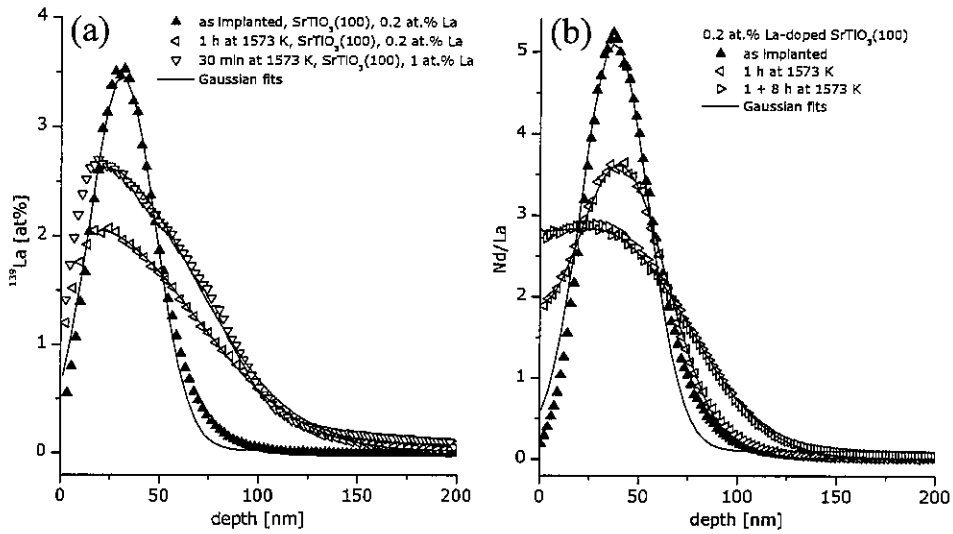


**Figure 3.** SIMS depth profiles of (a) La and (b) Nd. The La concentration was determined by normalizing to the natural background of the samples, which was subtracted afterwards.

Hence, under the assumption that beam damage decelerates the La tracer diffusion in the depth layer of $x \leq R_p$, only the part of $x > R_p$ of the La depth profiles was used to fit the data to Eq. 4. The Nd profiles were fitted to Eq. 5.

The results are compiled in Fig. 4. The diffusivities increase with the donor content, indicating that La and Nd diffusion takes place via Sr vacancies. As is expected for a cubic system, no dependence on the crystal orientation is found. Furthermore, a time dependence is observed. It is unlikely that this effect is related to thermal recovery, which should take place in much shorter time than the chosen experiment durations. Instead, we believe that this phenomenon is related to the space charge surface layer postulated by Meyer et al. [7]. Analogous to O diffusion, local space charge and defect concentration gradients lead to an enhancement of the La and Nd diffusivities in direction of the surface. Compared to La, the Nd diffusion coefficients are generally about an order of magnitude lower, indicating that in spite of the close relationship of the two elements, Nd may not be used as a direct analogue for La. In general, the measured diffusion coefficients are several orders of magnitude lower than the O tracer diffusion coefficients found in the literature, which range between $10^{-10}$ to $10^{-13}$ cm$^2$/s (T = 1573 K, x = 0 nm), depending on the dopant concentration [11]. Neglecting defect clusters, a cation vacancy mediated transport of the (dopant) tracer yields $D_{dopant} \cong 0.5 D_{V_{Sr}''}$ (see Eq. 1 and the relation $D_i \cdot c_i = D_v \cdot c_v$, i = cation, v = vacancy), which is in good agreement with an experimental value for $D_{V_{Sr}''} \cong 6\times10^{-15}$ cm$^2$/s at T = 1573 K in 0.2 at.% Nb doped $SrTiO_3$ [7]. This supports the assumption that La diffuses via Sr vacancies.

## ACKNOWLEDGEMENTS

The authors would like to thank the Deutsche Forschungsgemeinschaft (DFG) for financial support under the DFG contracts BO 532/47 and MA 1893/2.

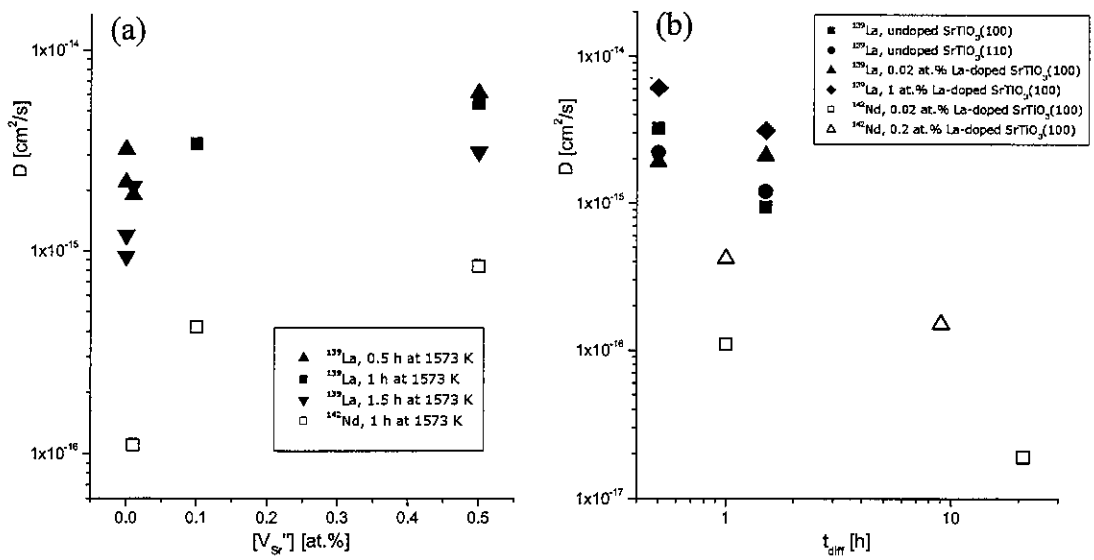


**Figure 4.** Values for the tracer diffusion coefficient D as a function of (a) Sr vacancy concentration (see Eq. 3), (b) annealing time.

## REFERENCES


1. R. Moos and K. H. Härdtl, *J. Am. Ceram. Soc.* **80**, 2549 (1997).
2. F. A. Kröger and H. J. Vink, *Solid State Phys.* **3**, 307 (1956).
3. K. Szot, W. Speier, U Breuer, R. Meyer, J. Szade, and R. Waser, *Surf. Sci.* **460**, 112 (2000).
4. Han Wei, W. Maus-Friedrichs, G. Lilienkamp, V. Kempter, J. Helmbold, K. Gömann, and G. Borchardt, *J. Electroceram.* **8**, 221 (2002).
5. S. N. Ruddlesden and P. Popper, *Acta Cryst.* **11**, 54 (1958).
6. A. Gunhold, K. Gömann, L. Beuermann, M. Frerichs, G. Borchardt, V. Kempter, and W. Maus-Friedrichs, *Surf. Sci.* **507-510**, 447 (2002).
7. R. Meyer, R. Waser, J. Helmbold, and G. Borchardt, *Phys. Rev. Lett.* (revised).
8. K. Szot and W. Speier, *Phys. Rev. B* **60**, 5909 (1999).
9. A. Gunhold, L. Beuermann, M. Frerichs, V. Kempter, K. Gömann, G. Borchardt, and W. Maus-Friedrichs, *Surf. Sci.* (2002) (in press).
10. A. Gunhold, K. Gömann, L. Beuermann, V. Kempter, G. Borchardt, and W. Maus-Friedrichs, *Anal. Bioanal. Chem.* (submitted)
11. J. Helmbold, PhD thesis, Technische Universität Clausthal, Germany (2001).
12. F. Poignant, PhD thesis, Université de Limoges, France (1995).
13. W. H. Rhodes and W. D. Kingery, *J. Am. Ceram. Soc.* **49**, 521 (1966).
14. M. J. Akhtar, Z.-U.-N. Akhtar, R. A. Jackson, and C. R. A. Catlow, *J. Am. Ceram. Soc.* **78**, 421 (1995).
15. R. Meyer, K. Szot, and R. Waser, *Ferroelectrics* **224**, 751 (1998)
16. H. Ryssel and I. Ruge, *Ion Implantation* (Wiley, Chichester, 1986), chapter 2.1.